Computational Dosimetry on Contact Currents from Charged Human Body

Toshihiro Nagai #, Akimasa Hirata#1, Osamu Fujiwara#2
#Nagoya Institute of Technology, Department of Computer Science and Engineering, Nagoya, Japan
[1]ahirata@nitech.ac.jp, [2]fujiwara@odin.nitech.ac.jp

***Abstract*— Contact current, defined as indirect effects of electromagnetic fields, flows a human body when contacting with an object such as a metal structure at a different electric potential, and may stimulate muscle and peripheral nerve. Thus, numerical analyses of electric fields induced by contact currents in a human body have been performed. Computational methods and evaluations of effects of transient field associated with contact currents have not yet been understood sufficiently. In the present study, we have simulated induced electric field in a human body due to contact current with dispersive FDTD method incorporated with a Japanese adult male model developed at National Institute of Information and Communication Technology. We compared FDTD calculations of body surface magnetic fields caused by contact current with measurements to validate our FDTD modeling, and then calculated induced peak electric field. As a result, we found that calculated and measured result of body surface magnetic fields are in fair agreement, confirming the validity of our FDTD modelling. The induced electric field becomes higher around the arm, while relatively lower in the central nerve systems.**

***Key words*: charged human body, contact current, FDTD simulation**

I. Introduction

There has been increasing public concern about adverse health effect due to electromagnetic waves. Contact current would cause indirect effects of electromagnetic fields on humans [1, 2]. In the frequency range up to approximately 100 kHz, the flow of electric current may result in the stimulation of muscles and/or peripheral nerves. The feature of the contact current is that the induced current in the body largely depends on the current pathway, which is largely different in actual scenarios.

Before the human touches conducting object with different electrical potential, transient current or spark discharge occurs, resulting in micro-shock to humans. Discharges associated with a static field (as in the case of walking on a carpet) are non-repetitive phenomena, whereas repetitive for time-varying fields (50 or 60 Hz). Steady contact current flows in the human once the human in time-varying fields touches conducting object with different potential.

Computation of induced electric field/current has been conducted for contact current [3-7]. In particular, Dawson *et al* have reported that contact current at steady state produces electric fields in tissue greater than those induced by external electric and magnetic fields [3]. Transient component of contact current, or spark, has been investigated in [4-6]. Amoruso *et al.* [4] investigated the induced current in a human body based on a circuit model with lumped parameters, and then evaluated induced currents in several human body parts. In that model, induced current in specific nerve tissues cannot be calculated, since the model is comprised of several body parts and the anatomy composition of the model is not taken into account. Okoniewska *et al*. implemented an FDTD scheme to evaluate transient component of the contact current in an anatomically-based human body model. In their modeling, the standard current for contact discharge prescribed in IEC (International Electrotechnical Commission) standard 61000-4-2 [5] was injected from the forefinger, which does not simulate any ESD events from charged human bodies. In addition, the human tissues were simplified as non-dispersive. In order to overcome this difficulty, the same group discussed in the frequency domain. The injection current, however, was the same as that prescribed in IEC standard. In these circumstances, induced electric field/current in the anatomically-based model has not yet been clarified [6].

In the present study, we have conducted computational dosimetry in the human due to transient component of contact current. The anatomically-based Japanese adult male model named TARO [8] was used in this investigation. We also conducted measurement of contact current and resultant body surface magnetic fields in order to validate our dispersive FDTD modeling.

II. Computational Models and Methods

A. Measurement Setup

The experimental condition considered is shown in Fig. 1 (a), which was almost identical in [9]. This setup is to measure a discharge current and induced surface magnetic fields due to the approach of a metal piece from a charged human body. For the metal bar, we used a metalic tip electrode with a curvature of 4 mm (8 mm in diameter), which is being employed as a current injection electrode of an ESD-gun. An aluminum plate (1m-by-2m) was placed as a ground vertically on a square aluminum plate with a side of 1 m. As shown in Figure 1(a), the input impedance of the target is $1+j0\ \Omega$ for calibrating current by IEC. Then, it was connected through a coaxial cable with a characteristic impedance of Z_0 (=50Ω) to a digital oscilloscope with a frequency band of 12 GHz and a sampling frequency of 40 GHz.

B. Computational Models and Methods

The human body model used is based on the adult male model named TARO [8]. This model has been developed with the magnetic resonance images of a volunteer whose height

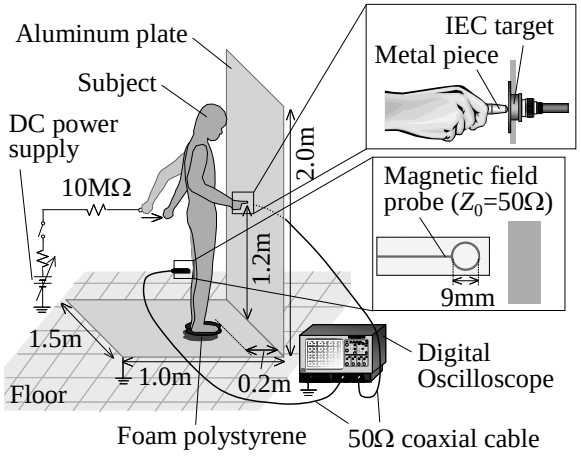

(a)

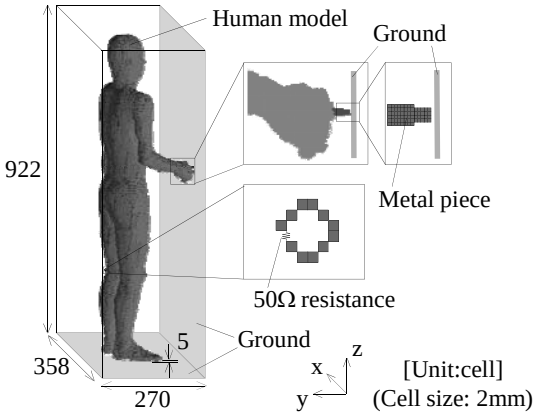

(b)

Fig. 1 (a) Setup for measuring contact currents and magnetic near-fields on body surfaces through a hand-held metal piece from a charged human and (b) corresponding FDTD model.

and weight of the model are 1.73 m and 65 kg for males. The voxels were rescaled to 2 mm cubes and segmented to define 51 discrete organs. The right arm and fingers of this body model was bent manually to match the experimental condition in Fig. 1.

The Finite-Difference Time-Domain (FDTD) method was used for investigating the electromagnetic interaction with a charged human body. Thus, the side length of the FDTD cell was chosen as 2 mm, which coincides with the human model resolution. The human tissues were assumed to obey to a four-pole Debye or dispersive medium. Then, its electrical constants were determined by the method of least squared in comparison with measured data in [10] in the frequency region between 10 kHz and 10 GHz. Even though we chose the lower frequency as 10 kHz, our computation is expected to be reasonable for much lower frequency. This is because the conduction current is dominant below 10 kHz and the tissue conductivity is almost uniform below this frequency. For truncation of the computational region, 12-layered PML (perfect matched layer) was used.

The contact of charged human body with conducting plate was simulated as an equivalent voltage source with one cell

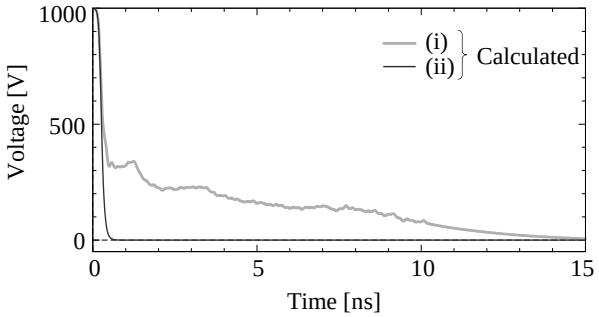

Fig.2 The waveform of excitation voltage at the human-plate gap: (i) estimated from measured contact current and the human body impedance, and (ii) assumed as an ideal switch.

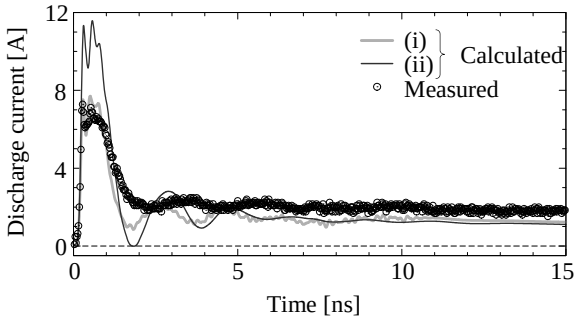

Fig.3 Computed and measured contact currents.

gap. We consider two schemes for providing excitation voltage: (i) estimated from measured discharge current and the frequency characteristics of human body impedance [8], and (ii) assumed as an ideal switch (or shorted). A lumped resistance of 1 Ω was inserted in the corresponding cell to model the IEC target. In order to simulate the shielded-loop probe, metallic loop with inner and outer radius of 9.0 mm and 10.0 mm, respectively, and one-cell gap with the impedance of 50 Ω was inserted. The charged voltage of human was chosen as 1 kV.

III. VALIDATION

Fig. 2 shows the waveform of excitation voltage at the human-plate gap. The notations of (i) and (ii) correspond the excitation schemes defined in the previous section. As seen from this figure, the human voltage drops instantly to the ground level for the scheme of (i), whereas it decreases gradually for the scheme of (ii) relative to (i). In addition, the effective descent of the voltage for (ii) is smaller than that for (i) [8]. The reason for this difference could be attributed to the arc and glow, following the spark. They are not taken into account in (ii), since the spark is assumed to fully develop. Computed contact currents for the excitation voltage in Fig.2 are shown in Fig. 3, together with measurement. From Fig. 3, the waveform computed with (i) is in good agreement with the measured one, whereas that with (ii) is 50% larger than the measurement. The reason for the difference between (ii) and measurement is attributed to the arc and glow followed by the spark, as mentioned above.

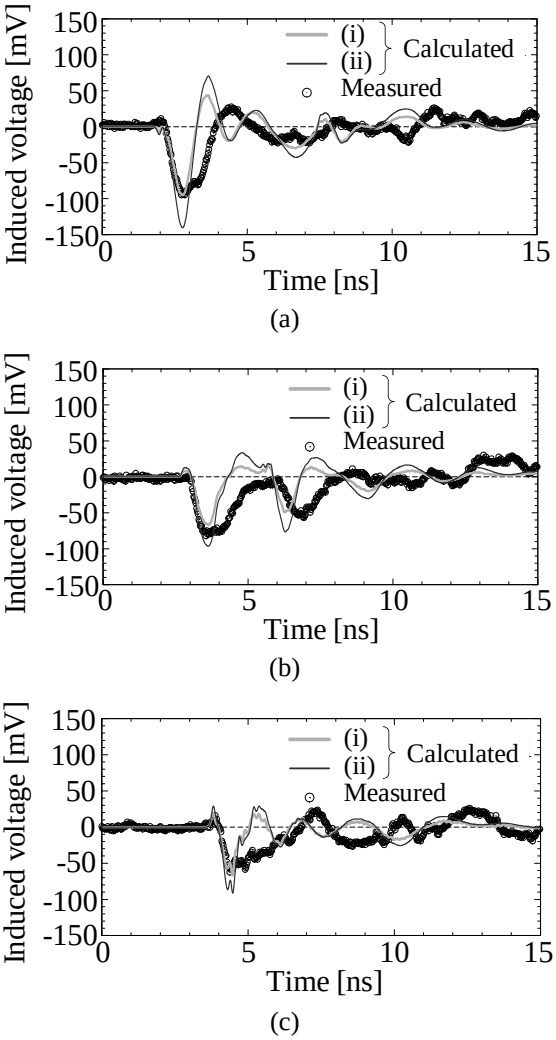

Fig. 4. Waveforms of induced voltage with the magnetic probe at (a) the lower back, (b) the rear of left knee, and (c) the rear of the left ankle.

Fig. 4 shows the waveform of induced voltage with the magnetic probe. The magnetic probe was chosen to locate at (a) the lower back, (b) the rear of left knee, and (c) the rear of the left ankle. At each location, we measured both vertical and horizontal components of magnetic field. From this figure, the shapes of the waveforms resemble one another. However, some difference was observed in the peak amplitudes between measurements and values computed by the excitation voltage of (ii), which is discussed above. Fair agreement was observed in the times when the peaks appear. This difference is thought to be mainly due to the difference in the body dimension as well as anatomically composition between the computational model and volunteer. Note that the height and weight of the human volunteer were 1.77 m and 60 kg, respectively while those are 1.73 m and 65 kg for the computational model. Due to the lack of space, we did not present the waveforms for horizontal component. Similar tendency was observed for the horizontal polarization.

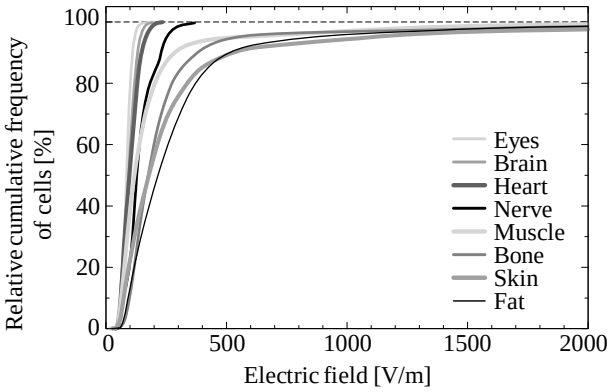

Fig. 5. Relative cumulative frequency of cells for time-peak electric field.

Table 1. 99th and average value of induced electric field in different tissues and organs.

Tissue	E_{99} [V/m]			E_{avg} [V/m]		
	(i)	(ii)	Δ[%]	(i)	(ii)	Δ[%]
Blood	303	372	-18.5	78	113	-30.9
Bone	2364	3460	-31.7	204	286	-28.6
Brain	113	167	-32.3	64	95	-32.4
Eyes	92	137	-32.7	56	87	-34.8
Fat	1868	2710	-31.1	237	337	-29.6
Heart	129	196	-34.6	69	102	-32.5
Muscle	1176	1718	-31.6	140	200	-30.1
Nerve	230	317	-27.6	99	141	-29.8
Skin	2686	3827	-29.8	256	359	-28.9
Whole body	1349	1967	-31.4	170	242	-29.8

IV. Computational Dosimetry

From the discussion in the last section, we refereed to the scheme (i) as actual evaluation and (ii) as overestimation from the standpoint of electromagnetic dosimetry. For these two schemes, we computed induced electric field in different tissues/organs of the human model. The induced electric field corresponding to the current density is a metric to assess the nerve stimulation. Note that the specific energy absorption is used for a metric for evaluating the thermal evaluation. However, the energy emitted from one discharge is much smaller than the threshold values [7]. For this reason, our discussion is concentrated on induced electric field. Note that induced electric field, especially for its 99th percentile is being discussed as a metric of nerve stimulation, instead of current density averaged over 1 cm^2 [2].

Our computation has been truncated at 190 ns when the amplitude of contact current becomes 1/100 as compared to its peak value. For each voxel in the human models, the time-peak value of induced electric field are stored till 190 ns, and then 99th percentile and mean values are calculated for different tissues/organs. Table 1 lists the 99th percentile and average values of induced electric field in different tissues/organs. Figure 5 shows the relative cumulative frequency of cells for different tissues and organs for the

scheme (ii). From Table 1, the 99th percentile and average values of induced electric field calculated with the scheme (ii) is 30% larger than those with the scheme (i). The induced fields become large in the order of the skin, bone, fat, and muscle. From Fig. 5, the relative cumulative frequency of cells reaches steeply at 90% or more, suggesting that the induced field is localized. The 99th percentile values of induced electric field were 167 V/m and 137 V/m in the brain and eyes, while those are 317 V/m and 196 V/m in the nerve and heart. The former two values are smaller than the latter, since the head is not located on the current path, as is the same as the steady contact current at 50/60 Hz [4]. They all are smaller than those in the muscle by a factor of 10. The current would decrease rapidly away from the right hand. The time when the peak induced field was stored was smaller than 15 ns.

In order to evaluate the induced fields in peripheral nerve tissue, especially for the skin, a formula for the threshold of perception has been used [11]:

$$E_T = \frac{1}{1-e^{-t/\tau_e}} \times E_0 \quad (1)$$

$$E_T = \begin{cases} \dfrac{\tau_e}{t} \times E_0 & t \le \tau_e \\ E_0 & t > \tau_e \end{cases} \quad (2)$$

where (1) is the original equation and its recurrent form is given by (2). Note that E_T denotes the threshold electric field, E_0 the rheobase, τ_e the strength-duration time constant. For the peripheral nerve tissue, E_0=6.15 V/m and τ_e =149 μs. This threshold has not been referenced as the rationale in the international guidelines [1], while some related description based on these equations can be found in [12]. In addition, the reference level for the continuous injection current has been regulated in [1].

The field induced in the skin of the figure was found not to satisfy for the discharge voltage of a few kilovolts for threshold (2). This is comparable to the perception threshold reported in [1], suggesting the usefulness of our computational method. However, it is difficult to determine the pulse duration of contact current. The parameters for E_0 and τ_e have not been well supported by measurements. Thus, quantitative discussion on the threshold field induced in peripheral nerve tissue remains as future work.

V. Summary

In the present study, we have simulated induced electric field in a human body due to contact current with the FDTD method incorporated with a Japanese adult male model developed at National Institute of Information and Communication Technology. We compared FDTD calculations of body surface magnetic fields caused by contact current with measurements to validate our FDTD modeling, and then calculated induced peak electric field. As a result, we found that calculated and measured result of body surface magnetic fields are in fair agreement, confirming the validity of our FDTD modeling. The induced electric field becomes higher around the arm, while relatively lower in the central nerve system.

For ultra-short electromagnetic pulse, such as transient component of contact current, the basic restriction has not been regulated. On the other hand, continuous contact current, the reference level has been regulated for preventing pain and burn. The field induced in the skin of the figures was found not to satisfy for the discharge voltage of a few kilovolts for threshold (2). The parameters for E_o and τ_e, however, have not been well supported by measurements. Thus, quantitative discussion on the threshold field induced in peripheral nerve tissue remains as future work

References

[1] ICNIRP, (International Commission on Non-Ionizing Radiation Protection), "Guidelines for limiting exposure to time-varying electric, magnetic, and electromagnetic fields (up to 300 GHz)," *Health Phys.*, vol.74, pp. 494-522, 1998

[2] World Health Organization, Environmental Health Criteria 238, pp.110-111, 203-206, 2007.

[3] V. Amoruso, M. Helali, and F. Lattarulo, "An improved model of man for ESD Applications," *J. Electrostat.*, vol.49, pp.225-244, 2000.

[4] T. W. Dawson, K. Caputa, M. A. Stuchly, R. Kavet, "Electric fields in the human body resulting from 60-Hz contact currents," *IEEE Trans. Biomed. Eng.*, vol.48, no.9, pp.1020-1026, 2001.

[5] E. Okoniewska, M. A. Stuchly, M. Okoniewski, "Interactions of electrostatic discharge with the human body," *IEEE Trans. Microwave Theory Tech.*, vol.52, pp.2030-2039, 2004.

[6] T. W. Dawson, M. A. Stuchly, R. Kavet, "Electric fields in the human body due to electrostatic discharge", IEEE Trans. Biomed. Eng., Vol.51, No.8, pp.1460-1468, Aug.2004.

[7] T. Nagai, A. Hirata, and O. Fujiwara, "FDTD simulation of contact currents from charged human body," IEICE Technical Report, EMCJ2008-38, July 2008.

[8] T. Nagaoka, S. Watanabe, K. Sakurai, E. Kunieda, S. Watanabe, M. Taki, and Y.Yamanaka, "Development of realistic high-resolution whole-body voxel models of Japanese adult males and females of average height and weight, and application of models to radio-frequency electromagnetic-field dosimetry", *Phys. Med. Biol.*, vol.49, pp.1-15, 2004.

[9] I. Mori, Y. Taka, and O. Fujiwara, "A circuit approach to calculate discharge current through hand-held metal piece from charged human-body," *Proc. 2005 Int'l Conf. Electromagent. Compat.*, Phuket, Thailand, 4A-4, July 2005.

[10] C. Gabriel, "Compilation of the dielectric properties of body tissues at RF and microwave frequencies", Brooks Air Force Technical Report AL/OE-TR-1996-0037, 1996.

[11] J. P. Reilly, "Mechanisms of electrostimulation: application to electromagnetic field exposure standards at frequencies below 100 kHz", P. Chadwick, C. Gabriel (eds.), The International EMF Dosimetry Handbook, http://www.emfdosimetry.org.

[12] IEEE Standard for Safety Levels with Respect to Human Exposure to Electromagnetic Fields, 0-3 kHz, IEEE Std C95.6-2002, 2002.